4th Asia Pacific Conference of the Prognostics and Health Management,
Tokyo, Japan, September 11 – 14, 2023 OS01-03

Study on the Estimation of Concrete Defects Volume on Dam Body Surface

Akira Ishii[1], Hiroaki Sugawara[2], and Masazumi Amakata[3]

[1,2,3] *Yachiyo Engineering Co., Ltd., Taito-ku, Tokyo, 111-8648, Japan*
akri-ishii@yachiyo-eng.co.jp
sugawara@yachiyo-eng.co.jp
amakata@yachiyo-eng.co.jp

ABSTRACT

To maintain the safety and functionality of dams over the long term, it is necessary to make inspections more labor-saving and efficient using the latest technology and to improve the sophistication of inspections based on data. Although dam inspections cover a wide range of items, this study focuses on the continuous monitoring of popouts, a phenomenon of concrete deterioration occurring on the surface of a dam body. It is difficult to predict whether a popout will occur from information on the body surface of the dam, owing to the generation mechanism of the popout. The number of popouts was monitored over time; however, no examples of shape changes were monitored over time. Advancements in various digital technologies are required to accurately evaluate changes in the dam body's surface over time; therefore, in this study, three-dimensional (3D) point-cloud data is created by the Structure from Motion (SfM) from images captured by a Unmanned Aerial Vehicle (UAV) of the concrete defect area due to the popout in an arch dam in the Tohoku region of Japan. The volume of concrete defects of a popout in each of two different periods was calculated by estimating the plane shape of the surface of the dam body. In addition, the shapes of two popouts were compared to confirm the possibility of predictive signs of change.

1. INTRODUCTION

1.1. Background

In Japan, daily inspections, periodic inspections every three years, and comprehensive inspections every 30 years are conducted to maintain the safety and function of dams over the long term. Although dam inspections cover a wide range of investigation areas and items, it is important to conduct inspections and maintenance management even under social structures, such as aging infrastructure, declining population and lack of personnel, and natural environments, such as frequent heavy rainfall and rising temperatures, which are expected to undergo significant changes in the future.

Conventionally, inspection of a dam body surface is conducted by inspection engineers using temporary scaffolding, gondolas, rope access, or other direct access methods. Dam inspection entails some challenges such as work preparation costs for access, limited work periods owing to non-flood periods, hazards from working at heights, and long work hours owing to extensive inspections. In addition, the results of the inspection survey are not accurately captured over time in terms of the location, shape, and quantity of deterioration information owing to the digitization of handwritten notes on drawings and differences in the evaluation of inspection results depending on the inspection engineer's competence. Therefore, new inspection and maintenance management methods that use technologies such as Information and Communication Technology (ICT) and Artificial Intelligence (AI) are required to replace human resources and analog inspections. Currently, maintenance management is based on post-inspection results. However, in the future, data accumulation is expected to lead to data-driven preventive maintenance management.

1.2. Purpose

As shown in Figure 1, popout, one of the concrete deterioration phenomena focused on in this study, implies that the concrete surface peels off in the shape of a thin plate. If the concrete surface contains low-quality aggregates with high water absorption, the internal expansion pressure increases, thereby causing the extrusion of the aggregates. Frost damage, wherein water in the concrete repeatedly freezes and thaws, contributes to this phenomenon. Therefore, continuous monitoring is required.

The authors are researching a method to objectively and quantitatively evaluate the deterioration status of the dam body surface through AI-based image recognition (Yasuno, Fujii, and Amakata, 2019)(Yasuno, Ishii, Fujii, Amakata, and Takahashi, 2020) using images captured by autonomous UAV flights. In above these research, the popouts can also be counted as the number of popouts that occur on the surface of the dam body. Moreover, changes in the number of popouts can be confirmed by photographing the dam over time. Once a popout occurs, it is theoretically considered not to expand. However, the images of the dam body's surface can only confirm the presence or absence of anomalies on the dam body's surface. It is unclear how many low-quality aggregates exist in the dam body concrete, and the actual state of deterioration in the depth direction has not been confirmed. Higher-order information is required to estimate the signs of popout occurrence and to confirm the expansion in the depth direction over time after popout occurrence. Therefore, as a fundamental study, this study reconstructed the 3D shape of each popout from the aerial images captured by UAVs close to the dam body surface at two different periods. The volume of concrete defects owing to each popout was then estimated, and the two popout shapes were compared.

The remainder of this paper is organized as follows: Section 2 introduces the method for measuring the shape of the popout in related work. Section 3 presents the proposed methodology applied to the estimation of the concrete defect volume and a comparison of the popout shapes. Section 4 validates the proposed methodology using field data. Finally, the conclusions and future work are discussed in Section 5.

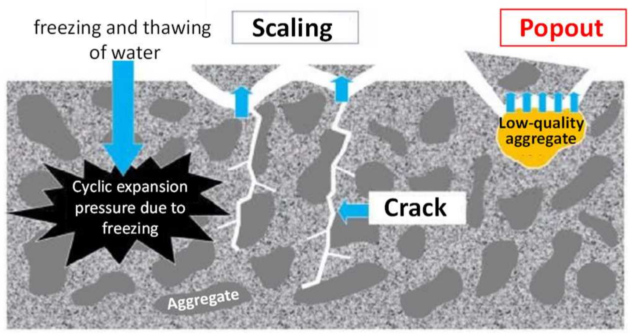

Figure 1. Popout generation mechanism.

2. Measurement of Popout Shape

There are three possible methods for measuring the popout shape on the surface of a dam body: measurement by an inspection engineer, measurement using Light Detection And Ranging (LiDAR), and 3D reconstruction using photogrammetry. An overview of each method is provided below.

2.1. Inspection Engineer

To access the surface popout of the dam body, inspection technicians must assemble temporary scaffolds or use ropes or gondolas. Even if the popout location is accessed using such a technique, it is difficult to record the popout shape because it is complex, and there is no technique to measure or trace it completely on the spot.

2.2. LiDAR

The authors realized autonomous navigation of a UAV using a total station navigation, total station is surveying instrument, in the vicinity of a dam body, where Global Navigation Satelite System (GNSS) could not be received properly. (Ishii, Yasuno, Amakata, Sugawara, Fujii and Ozasa, 2020). This method can obtain accurate flight position information without a high-precision Inertial Measurement Unit (IMU). Therefore, the digital camera mounted on the UAV was changed to a LiDAR to enable point cloud measurement by the UAV, even in a non-GNSS environment. Figure 2 shows the results of the measurement of a popout near the center of the dam body surface using this method with a LiDAR (Velodyne, VLP-16-LITE) mounted on a UAV. Owing to the variability of the LiDAR measurements, the surface of the dam body cannot be represented as the only surface. It is difficult to represent the popout shape because of the need for noise processing and adjustments using fixed or validation points.

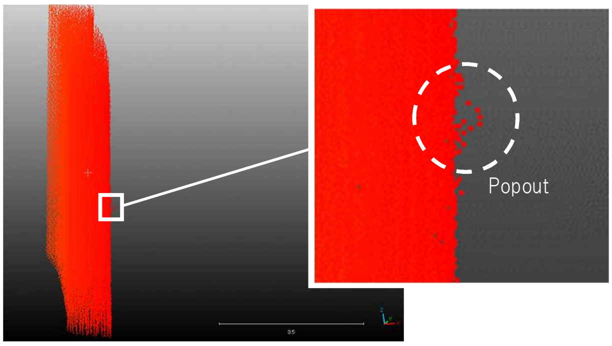

Figure 2. LiDAR measurement results in the vicinity of the popout on a sliced section of the dam body.

2.3. Photogrammetry

The 3D dam shape and aerial image positions are obtained from consecutive and overlapping aerial images captured by a UAV using SfM. Feature points are then automatically extracted from each aerial image, and the 3D shape of the dam body surface is reconstructed by matching the feature points between the images. Although the point-cloud data for the dam body's surface are uniquely determined, the reconstructed dam body's surface shape differs depending on the brightness, hue, and appearance of the image while capturing it as it is not possible to set fixed points or validation points on the dam body's surface (Ishii, Sugawara, Fujii and Amakata, 2023). However, because the dam body surface is constructed using clean point-cloud data, this study used a 3D geometry of the dam body surface reconstructed by photogrammetric methods.

3. METHODOLOGY

3.1. Estimation Method of Concrete Defects Volume

This section describes the procedure for estimating the volume of concrete defects caused by popouts. The procedure is as follows:

1. 3D reconstruction of the dam body surface, including the popout, by SfM using aerial images. Next, the point-cloud data of the popout were extracted from the reconstructed 3D shape. The extraction of the point-cloud data of the popout was performed because the dam is an arch-type, and the plane shape of the dam body's surface is complex.
2. Estimation of the plane shape of the dam body surface. From the point-cloud data of the extracted popout area, the variables of the plane equation in Eq. (1) of the dam body surface were estimated by Random Sample Consensus (RANSAC).
$$aX + bY + cZ + d = 0 \tag{1}$$
3. Calculation of the distances between the estimated planes using Eq. (1) and each point of the pop-out using the point and plane formulas in Eq. (2).
$$d_i = \frac{|ax_i + by_i + c_i + d|}{\sqrt{a^2 + b^2 + c^2}} \tag{2}$$
4. Calculation of the unit vectors r and r' of the normal values of the estimated plane using Eq. (1) and XY plane, respectively.
5. Calculation of angle θ from the unit vectors r and r' using Eq. (3).
$$\theta = arcos \frac{\vec{r} \cdot \overrightarrow{r'}}{|\vec{r}| \cdot \left|\overrightarrow{r'}\right|} \tag{3}$$
6. Calculation of the unit vector $n = (n_1, n_2, n_3)$ of the axis of rotation from the unit vectors r and r' using the outer product.
7. Rotation of the popout point-cloud data r around the rotation axis by θ using the Rodriguez rotation formula listed in Eq. (4).
$$r' = R_n(\theta)r \tag{4}$$
where rotation matrix $R_n(\theta)$ in Eq. (4) is expressed by Eq. (5). Subsequently, all rotated points are projected horizontally onto the XY plane.
$$R_n(\theta) = \begin{pmatrix} n_1^2(1-cos\theta)+cos\theta, & n_1n_2(1-cos\theta)-n_3sin\theta, & n_1n_3(1-cos\theta)+n_2sin\theta \\ n_1n_2(1-cos\theta)+n_3sin\theta, & n_2^2(1-cos\theta)+cos\theta, & n_2n_3(1-cos\theta)-n_1sin\theta \\ n_1n_3(1-cos\theta)-n_2sin\theta, & n_2n_3(1-cos\theta)+n_1sin\theta, & n_3^2(1-cos\theta)+cos\theta \end{pmatrix} \tag{5}$$
8. Calculation of the average area A_i for each point. The average area A_i is calculated by dividing the space by a voronoi division based on the points distributed in the XY plane, calculating the area of each region delimited by each point, and averaging the area of each region.
9. Calculation of the concrete defect volume V due to the popout using Eq. (6).
$$V = \sum_{i=1}^{m} (A_i \times d_i) \tag{6}$$

3.2. Comparison of Popout shape

The closest iterative Points (ICP) algorithm (Paul & Neil, 1992) was used for the alignment process between the point clouds. The procedure is as follows:

1. Nearest neighbor search: For each point in point group P_k, which is the converted source data, the corresponding point in point group X, which is the destination data, is searched. The collection of corresponding points is defined as Y_k, where k is the number of iterations of each step of the ICP algorithm, and the numbers of P_k and Y_k points N are the same. The Euclidean distance between the two points is then set to $d(r_1, r_2)$, and the distance between a specific point p and a point-cloud data group $A = \{a_i\}, \mathrm{i} = 1, \ldots, N_a$ consisting of N_a points, is set to $\mathrm{d}(p, A) = \min_{i \in \{1, \ldots N_a\}} d(p, a_i)$. For all points in P_k, the nearest neighbor points to X are searched in the kd-tree, which corresponds to the point set $Y_k = C(P_k, X)$.
2. Estimation of rigid-body transformation: The rigid-body transformation that minimizes the position error between two-point clouds is estimated using the P_k and Y_k covariance matrices. The centers of gravity of the two-point groups, P_k and Y_k are computed in Eq. (7), respectively: The covariance matrices are expressed by Eq. (8).
$$\vec{u}_p = \frac{1}{N}\sum_{i=1}^{N} p_{i,} \quad \vec{u}_y = \frac{1}{N}\sum_{i=1}^{N} y_{i,} \tag{7}$$
$$\begin{aligned} \Sigma_{py} &= \frac{1}{N}\sum_{i=1}^{N}\left[(p_i - \vec{u}_p)(y_i - \vec{u}_y)^T\right] \\ &= \frac{1}{N}\sum_{i=1}^{N}[p_i {y_i}^T] - \vec{u}_p\vec{u}_y^T \end{aligned} \tag{8}$$
Then, the 4×4 symmetric matrix $\mathrm{Q}(\Sigma_{py})$ shown in Eq. (9) is calculated.

$$\mathrm{Q}(\Sigma_{py}) = \begin{bmatrix} tr(\Sigma_{py}) & \Delta^T \\ \Delta & \Sigma_{py} + \Sigma_{py}^T - tr(\Sigma_{py}) I_3 \end{bmatrix} \tag{9}$$

where $tr(\Sigma_{py})$ is the sum of the diagonal components Σ_{py}, $\Delta = [A_{12} A_{31} A_{12}]^T$ is a vector consisting of $A_{ij} = (\Sigma_{py} - \Sigma_{py}^T)_{ij}$, and I_3 is a 3×3 unit matrix. As the eigenvector for the largest eigenvalue of $\mathrm{Q}(\Sigma_{py})$ corresponds to $q_R = [q_0 q_1 q_2 q_3]^T$, the translation component can be calculated using Eq. (10).

$$q_t = \vec{u}_y - R(q_R)\vec{u}_p \tag{10}$$

3. Update of the object posture. The converted source point-cloud data P_k is updated.
4. Convergence judgment: If there is no convergence, the process returns to 1. Steps 1–3 are repeated until the convergence conditions are satisfied. The convergence condition is satisfied when one of the following conditions is satisfied:
   - The squared error of the converted source and destination point-cloud data is less than the threshold value.
   - Maximum number of iterations.
   - The amount of displacement between the k-1 step and k-step rigid-body transformations is below the threshold.

4. Results

4.1. Data Used for Verification

In an arch dam in the Tohoku region of Japan, numerous popouts of various sizes, ranging from the size of a human fist to that of a human head, were observed on the upstream and downstream surfaces of the dam body. Aerial images of the largest class of popouts in the center of the downstream surface of the dam body recorded with a resolution of approximately 2.0 mm/pixel by UAV autonomous navigation using total station navigation (Ishii et al, 2020) in 2019 and 2022 are shown in Figure 3. Although the shooting conditions are the same, the appearance of the popout is different because the shooting time is different.

4.2. Estimation Result of Concrete Defects Volume

The volume of the popout was estimated according to the procedure described in Section 3.1. The 3D shape of the dam body surface was reconstructed from the aerial image captured by the UAV using the SfM analysis software *Metashape*, and the popout shown in Figure 3 was manually extracted from the reconstructed 3D point-cloud data using the point-cloud processing software *CloudCompare*. The point-cloud data for the extracted popouts are shown in Figure 4. In Figure 4, the point-cloud data on the plane estimated using RANSAC are colored red for 2019 and blue for 2022. RANSAC uses the open3d library in Python, wherein the threshold of the maximum distance from the estimated plane was 0.01(m), the number of random sampling points was 1,000 points, and the number of times the plane was checked by sampling was 3,000 times to estimate the plane equations. In addition, because the aerial image was captured directly facing the dam body surface, the 3D reconstruction results in a point cloud that is curved into an arch shape, with the horizontal spacing widening and vertical lines becoming more prominent.

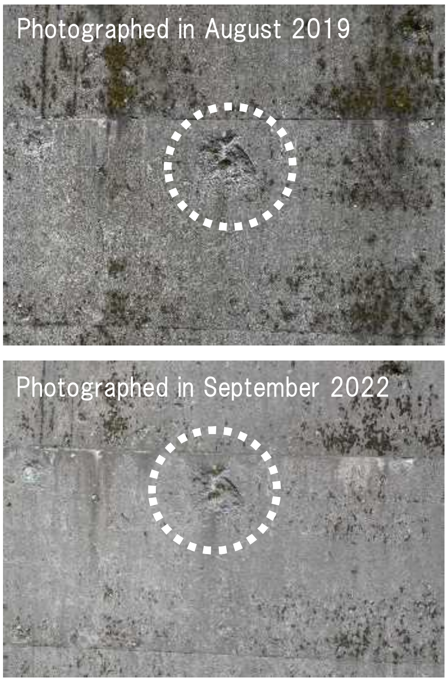

Figure 3. Aerial popout image.

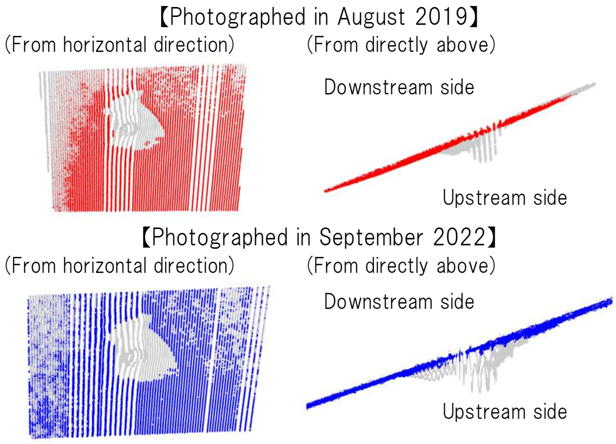

Figure 4. Bird's eye view of popout's point-cloud data

Table 1 shows the constants of the estimated plane equations, total number of point-cloud data, number of popout only point-cloud data (PCD), average and maximum distances between the estimated plane and popout points, average area per point, length of one side, and estimated volume. Here, the length of one side was the length of the side when the estimated volume was divided by the average distance, and the area was a square.

The estimated concrete defect volumes of the two popouts were almost the same. Although the absolute scale was unknown, the length of one side confirmed that it was of the same size as the largest class of popouts; therefore, the estimation method was considered correct.

Table 1. List of calculation results.

Item	2019 year	2022 year
Constants of the estimated plane equations	a: 0.9385 b: 0.3051 c: −0.1614 d: 52696.0546	a: 0.9336 b: 0.3154 c: −0.1701 d: 54068.8465
Number of PCDs (all)	111,627	117,369
Number of PCDs (popout only)	15,512	17,198
Average distances (m)	0.052	0.052
Maximum distances (m)	0.169	0.170
Average area per point (m^2)	0.113×10^{-4}	0.099×10^{-4}
Length of one side (m)	0.419	0.412
Estimated volume (m^3)	9.078×10^{-3}	8.778×10^{-3}

4.3. Results of Shape Comparison

Alignment of the point-cloud data for 2019 and 2022 was performed according to the ICP algorithm described in Section 3.2. The convergence conditions were set to a squared error of 0.003(m), the maximum number of iterations was 100, and the amount of moved displacement was below 0.0001(m).

Figure 5 shows the convergence of the distance error. It was confirmed that the distance error decreased monotonically and converged. Figure 6 shows the alignment results of the two-point clouds when convergence was achieved. Red shows the point cloud of the 2019 popout, and blue shows the point cloud of the 2022 popout, which are well-superimposed.

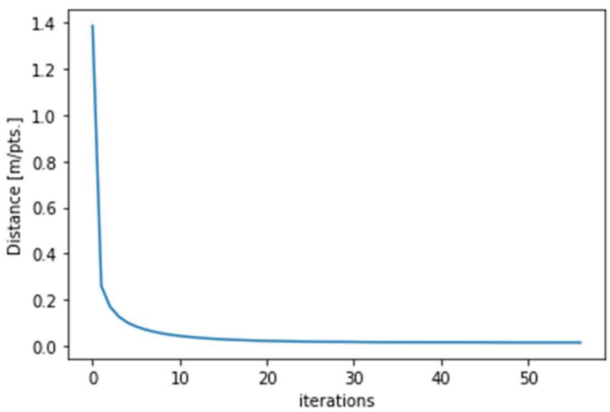

Figure 5. Convergence status of distance error.

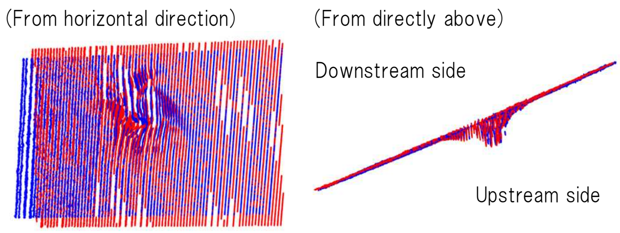

Figure 6. Aligment result of popout point-cloud data.

5. Conclusion and Future works

In this study, the 3D shape of each popout was reconstructed from the aerial images captured by UAVs in close proximity to the dam body surface at two different periods. The volume of concrete defects caused by each popout was estimated, and the two popout shapes were compared. The results showed that the concrete defect volumes of the two popouts were almost the same, and their shapes overlapped well, confirming that there were no significant shape changes during the three-year period from 2019 to 2022.

In future work, the topics to be examined are discussed below.

- Verification of estimation methods by comparison with field measurement results and theoretical values.
- Evaluation at different popouts.
- Improving the accuracy of the 3D reconstructed shapes using reference and fixed points.
- Automatic extraction of popouts scattered throughout dam body surface. In addition, the change in the shape of all the popouts will be investigated.
- To continue capturing aerial photography data in the future.
- Establishing a new method to predict the transition in the number of defects in the entire concrete as a new monitoring item.

References

Takato Yasuno, Junichiro Fujii, & Masazumi Amakata (2019). Pop-outs Segmentation for Concrete Prognosis Indices using UAV Monitoring and Dense Dilated Convolutions. *Proceedings of 12th International Workshop on Structure Health Monitering* (page 3175), September 10-12, California, USA. doi:10.12783/shm2019/32471

Takato Yasuno, Akira Ishii, Junichiro Fujii, Masazumi Amakata & Yuta Takahashi (2020). Generative Damage Learning for Concrete Aging Detection using Auto-flight Images. *2020 Proceedings of the 37th ISARC*, pp. 1211-1218. doi:10.22260/ISARC2020/0166

Akira Ishii, Takato Yasuno, Masazumi Amakata, Hiroaki Sugawara, Junichiro Fujii & Kohei Ozasa (2020). Autonomous UAV flight using the Total Station Navigation System in Non-GNSS Environments. *2020*

Proceedings of the 37th ISARC, pp. 685-692. doi:10.22260/ISARC2020/0096

Akira Ishii, Hiroaki Sugawara, Junichiro Fujii & Masazumi Amakata (2023), Study on How to Ensure the Accuracy of 3D Model in Digital Inspection of Dam Body Degradation Survey. *Intelligence, Informatics and Infrastructure Conference*. May 29, Tokyo, JAPAN. doi: 10.11532/jsceiii.4.2_38

Paul J. Besl, & Neil D. McKay (1992). Method for registration of 3-D shapes. *IEEE Transactions on Pattern Analysis and Machine Intelligence*, vol. 14, No.2., pp. 239-256. doi:10.1109/34.121791

Akira Ishii completed his B.S. and M.S. in civil engineering from Chuo University, Tokyo, Japan, in 2003 and 2005, respectively. He was employed as a civil engineer at INA Co., Ltd. from 2006 to 2012. Since 2013, he has been employed by Yachiyo Engineering Co., Ltd. and is currently working as a chief researcher at the Research Institute for Infrastructure Paradigm Shift in the same company.

Hiroaki Sugawara completed his B.S. and M.S. in traffic civil engineering from Nihon University, Chiba, Japan, in 1983 and 1985, respectively. He was employed as a civil engineer at Yachiyo Engineering Co., Ltd. from 1985 and is currently working as a deputy director at the Research Institute for Infrastructure Paradigm Shift.

Masazumi Amakata completed his B.S. in traffic civil engineering from Kyoto University, Kyoto, Japan, in 1997, and the Ph.D. degree from the Division of Environmental Science and Engineering, Graduate School of Natural Science and Technology, Kanazawa University, Ishikawa, Japan, in 2011. He was employed as a civil engineer at Yachiyo Engineering Co., Ltd. from 1997 and is currently working as a director at the Research Institute for Infrastructure Paradigm Shift.